

Preferential angular momentum transfer in state-to-state reactive scattering

S. H. Suck Salk* and R. W. Emmons

Department of Physics and Graduate Center for Cloud Physics Research, University of Missouri-Rolla, Rolla, Missouri 65401

(Received 2 January 1984)

An investigation is presented of how each angular momentum transfer during reaction contributes to a given state-to-state reactive transition. The new finding from this study is that some direct state-to-state reactive scattering systems which favor collinear configuration prefer the largest angular momentum transfer as a result of reactive collision and that such preference of the largest angular momentum transfer is shown to occur in both forward- and backward-peaked reactive scattering.

I. INTRODUCTION

Over the last ten years, both exact and approximate three-dimensional quantum mechanical methods¹⁻¹¹ have been proposed to study the rearrangement collision processes of the atom-diatomic molecule systems. Among the latter are the methods of Born approximation: plane-wave Born approximation (PWBA),⁵ distorted-wave Born approximation (DWBA),^{3(a),4,7} multichannel DWBA,^{3(c)} coupled-channel Born approximation (CCBA),¹⁰ and reactive infinite-order sudden approximation (RIOS).¹¹ Both the PWBA and DWBA work best for direct reaction (reactive scattering) processes. The superiority of DWBA to PWBA is generally pronounced at low collision energies. On the other hand, for indirect reaction processes which accompany intermediate states associated with the initial and final arrangement channels, the CCBA is a useful method which can replace both the PWBA and DWBA.

Unlike the case of nuclear reactions, the DWBA transition amplitude expanded in terms of angular momentum transfer in the elementary molecular reaction has the additional merit of directly obtaining a knowledge of the relative orientation between the rotational angular momenta of the product diatomic molecule and of the reactant diatomic molecule. Thus our method⁷ differs from other proposed molecular DWBA methods in this respect. The present study is the first application of such merit. The knowledge of relative orientation between the rotational angular momenta will render a better understanding regarding anisotropic properties of the hyperpotential surface involving three-body (triatomic) relative systems. Preferential angular momentum transfer in state-to-state reactive scattering will be subject to the nature of anisotropy in the potential surface.

Earlier we^{7(a)} pointed out the importance of angular momentum transfer in state-to-state reactive scattering processes. However, there has been no study regarding this problem for reactive transitions involving nonzero rotational angular momentum states for both the initial and final diatomic molecules. This is our first exploration in this area of reactive scattering for atom-diatomic molecule systems.

II. COMPUTED RESULTS AND DISCUSSIONS

For direct reactive scattering (that is, for ignorable pathways to intermediate states during collision) we find the fol-

lowing DWBA differential cross section:^{7,10}

$$\frac{d\sigma(n_b, j_b \leftarrow n_a, j_a)}{d\Omega} = \frac{\mu_a \mu_b}{2\pi\hbar^2} \frac{k_b}{k_a} \frac{1}{2j_a + 1} \sum_{j_m \geq m} |T_{jm}^{j_b j_a}|^2, \quad (1)$$

where the reduced transition amplitude is given by

$$T_{jm}^{j_b j_a} = \frac{2\pi}{k_b k_a} J(2j_a + 1)(2j_b + 1) \tau_{jm}^{j_b j_a}. \quad (2)$$

n_a (n_b) is the vibrational quantum number of the reactant (product) diatomic molecule. j_a (j_b) is the rotational angular momentum quantum number of the reactant (product) diatomic molecule. μ_a (μ_b) is the reduced mass and k_a (k_b) is the wave number for the initial (final) arrangement channel. J is the Jacobian of the coordinate transformation. $\tau_{jm}^{j_b j_a}$ is defined in Eq. (53) of Ref. 7. m is the z component of the angular momentum transfer j . $m \geq$ stands for m greater than or equal to 0. The incoherence in j enables us to examine the role of each angular momentum transfer and the relative orientations of rotational angular momenta.

The reactive systems we selected are $\text{He} + \text{H}_2^+ \rightarrow \text{HeH}^+ + \text{H}$ and $\text{F} + \text{H}_2 \rightarrow \text{HF} + \text{H}$. For both of these reactions, contribution of collinear configurations is significant. The former direct reaction process¹²⁻¹⁵ generally yields forward scattering and the latter, backward scattering.

For simplicity, we introduce a low-lying rotational transition from a vibrationally "hot" reactant ion, $\text{He} + \text{H}_2^+(n_a=2, j_a=1) \rightarrow \text{HeH}^+(n_b=0, j_b=1)$. For this state-to-state reactive scattering, the angular momenta transfer values are simply $j=0, 1$, and 2. Figure 1 shows the computed state-to-state reactive scattering angular distribution at the relative collision energy of 0.35 eV, employing the DIM potential surface of Kuntz.¹⁵⁻¹⁷ The scattered product ions are predicted to appear largely at forward directions while showing some backward scattering in the c.m. (center-of-mass) system. Other predicted state-to-state reactive transitions for $\text{H}_2^+(n_a=3)$ also showed more dominant forward-peaked scattering angular distributions at much higher collision energies of 1.0 to 3.6 eV. This trend is consistent with the observed angular distributions of Schneider *et al.*¹⁸ for the case of vibrationally hot reactant ion, $\text{H}_2^+(n_a=3)$. Here we would like to point out that the presently used DIM potential markedly differs from the more accurate SAI (spline-fitted *ab initio* surface^{19,20}) in the topology of the inner repulsive wall.¹⁴ As a consequence, the latter is known to yield vibrational enhancement unlike the former as was observed.¹⁴ Sathyamurthy, Duff, Stroud,

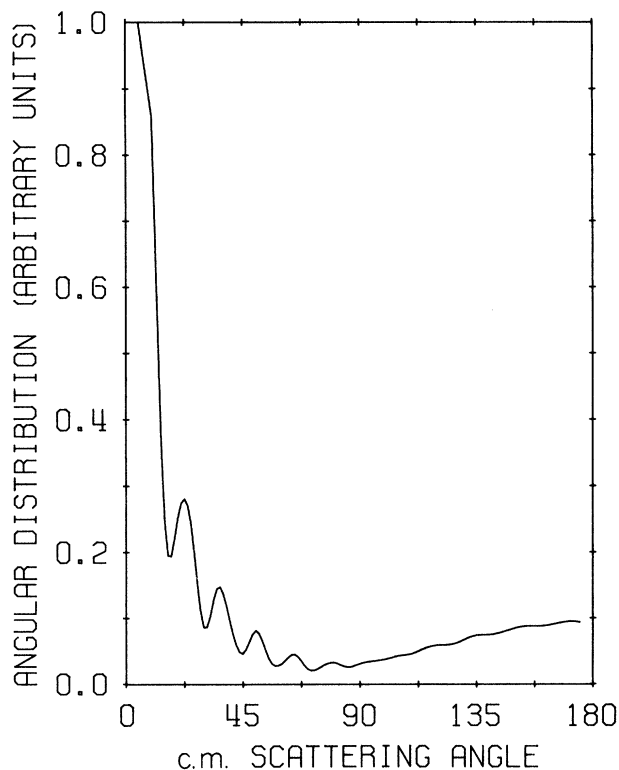


FIG. 1. State-to-state reactive scattering angular distribution for $\text{He} + \text{H}_2^+ (n_a=2, j_a=1) \rightarrow \text{HeH}^+ (n_b=0, j_b=1) + \text{H}$ at the collision energy of 0.35 eV.

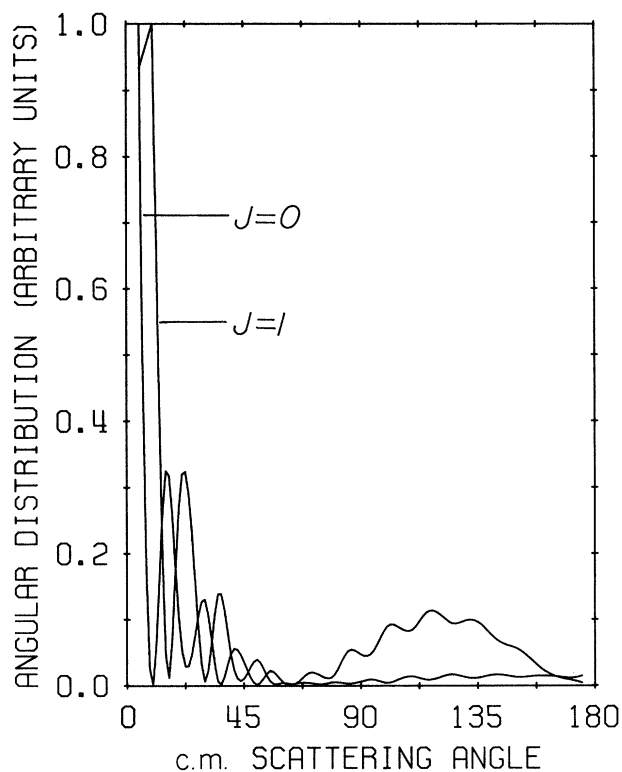


FIG. 2. Differential cross sections corresponding to the angular momentum transfer values of $j=0$ and $j=1$, respectively. Other definitions are the same as in Fig. 1.

and Raff¹⁴ note, however, almost no distinction between the two surfaces in the potential-energy contours, the height and location of the barrier minimum energy path, and its curvature, other than the difference mentioned above. The present paper does not deal with the vibrational enhancement,¹⁴ nor with the quantitative emphasis of absolute cross sections. Our major emphasis lies in the preference of angular momentum transfer as a result of anisotropic potential surface which has characteristics of collinearity. Since both the DIM and SAI potential surfaces have similar energy contours,¹⁴ our physical discussions will not be perturbed.

Due to the incoherence of the angular momentum transfer, j , the decomposition of the angular distribution above into the individual contributions of j is allowed. Figure 2 shows both the $j=0$ and $j=1$ contributions and Fig. 3, the $j=2$ contribution. All of the angular distributions corresponding to each angular momentum transfer show the dominance of forward scattering over backward scattering as shown in the figures. However, it is interesting to note the gradual enhancement of backward scattering as the angular momentum transfer increases, showing the local maximum at the backward c.m. scattering angle of 180° for the largest angular momentum transfer of $j=2$. The ratio of the integrated cross sections for each angular momentum transfer is $\tau(j=2):\sigma(j=1):\sigma(j=0) = 1:0.5:0.14$. This indicates that the state-to-state proton transfer reaction of present interest preferentially occurs via the largest angular momentum transfer. That is, the preferred direction of the rotational angular momentum of the scattered product ions HeH^+ is opposite to the direction of the rotational angular momentum of the reactant ion H_2^+ . This trend persisted at higher

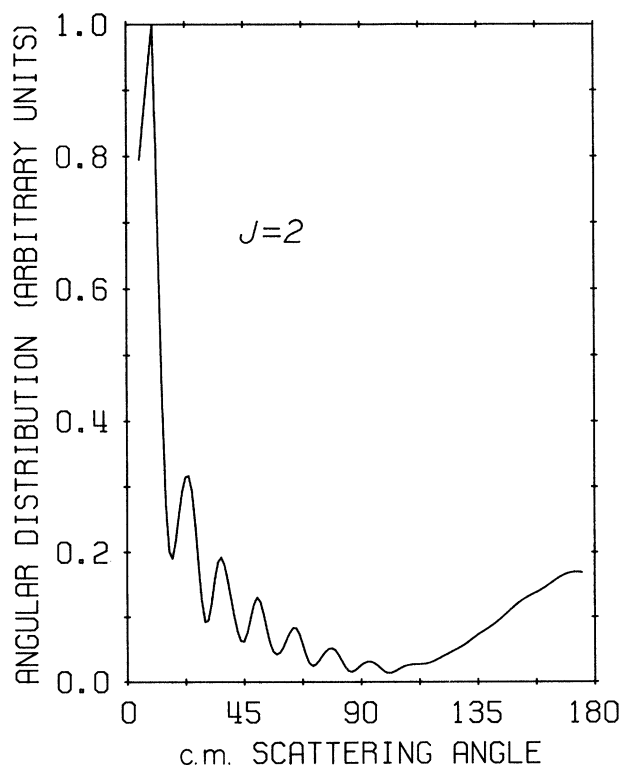


FIG. 3. Differential cross section corresponding to the angular momentum transfer, $j=2$. Other definitions are the same as in Fig. 1.

collision energies also. The predicted individual angular distributions for each angular momentum transfer j are highly oscillatory. However, the state-to-state angular distribution (the incoherent sum of each individual angular distribution corresponding to j) shows reduction in oscillatory structure as is seen in Fig. 1. This is seen to be caused by the dominant contribution of the largest angular momentum transfer during the reactive transition.

Although not presented here for brevity, our DWBA calculations using the Muckerman V potential surface²¹ for the FH_2 system also showed preferentially the largest angular momentum transfer as in the case of $\text{He} + \text{H}_2^+ \rightarrow \text{HeH}^+ + \text{H}$. The FH_2 potential surface is also well characterized by collinearity in configuration and generally yields backward scattering for various state-to-state reactive transitions^{7(b)} compared with forward scattering in the case of the HeH_2^+ system. Thus in both forward- and backward-scattering cases, we find the common characteristics of preferring the largest angular momentum transfer.

It is to be noted that the DWBA does not, in general, yield quantitatively accurate magnitudes for cross sections. Thus the DWBA methods are not recommended for chemical applications. However, it still remains to be seen how well these methods will serve for understanding physical mechanisms of elementary molecular reactions. The recent exact close-coupling study of Schatz and Kuppermann^{1(b)} shows great similarity in the structure of angular distributions between their exact method and the approximate DWBA method.^{4(b)} Both methods showed nearly superimposable backward-peaked structures (shape) in the state-to-state reactive scattering angular distribution of the H_3 system. Our predicted state-to-state angular distributions are dominantly characterized by the largest angular momentum

transfer, showing forward- or backward-peaked structures (shapes) which are generally consistent with observations.

III. CONCLUSION

In summary, we have (1) presented the first theoretic treatment of the role of angular momentum transfer on characterizing state-to-state reactive scattering angular distribution involving elementary molecular reactions; (2) found that some state-to-state reactive transitions which favor collinear configurations generally occur through the preference of the largest angular momentum transfer, thus indicating that the direction of the rotational angular momentum of the scattered product molecule tends to be preferentially opposite to that of the initial reactant molecule; (3) shown that for both the forward (as in $\text{He} + \text{H}_2^+ \rightarrow \text{HeH}^+ + \text{He}$) and backward scattering (as in $\text{F} + \text{H}_2 \rightarrow \text{HF} + \text{H}$), such preference of the angular momentum transfer remains unchanged; and (4) proposed that studies of the "weight" of each angular momentum transfer are important for understanding the consequences of anisotropic potential surface in reactive scattering. Finally, it will be of great interest to examine other state-to-state reactive transitions to find whether there exists any exception from the observations made above.

ACKNOWLEDGMENTS

This material is based upon work partially supported by the National Science Foundation Grant No. ATM-82-12328. He also thanks C. R. Klein, C. K. Lutrus, and D. E. Hagen for sharing scientific discussions on collision theories.

*Formerly known as S. H. Suck.

¹(a) A. Kuppermann and G. C. Schatz, *J. Chem. Phys.* **62**, 2502 (1975); (b) G. C. Schatz and A. Kuppermann, *ibid.* **65**, 4642 (1976).

²A. B. Elkowitz and R. E. Wyatt, *J. Chem. Phys.* **62**, 2504; **62**, 3683 (1975).

³(a) W. H. Miller, *J. Chem. Phys.* **49**, 2373 (1968); (b) **50**, 407 (1969); (c) L. M. Hubbard, S.-H. Shi, and W. H. Miller, *ibid.* **78**, 2381 (1983).

⁴(a) K. T. Tang and M. Karplus, *Phys. Rev. A* **4**, 1844 (1971); (b) B. H. Choi and K. T. Tang, *J. Chem. Phys.* **65**, 5161 (1975).

⁵A. Kafri, Y. Shimoni, and R. D. Levine, *Chem. Phys.* **13**, 323 (1976).

⁶B. C. Eu, *Mol. Phys.* **31**, 1261 (1976).

⁷(a) S. H. Suck, *Phys. Rev. A* **15**, 1893 (1977); (b) R. W. Emmons and S. H. Suck, *ibid.* **27**, 1803 (1983).

⁸C. L. Vila, D. J. Zvijac, and J. Ross, *J. Chem. Phys.* **70**, 5362 (1979).

⁹D. C. Clary and J. N. L. Connor, *J. Chem. Phys.* **75**, 3329 (1981).

¹⁰S. H. Suck, *Phys. Rev. A* **27**, 187 (1983).

¹¹J. Jellinek, M. Baer, and D. J. Kouri, *Phys. Rev. Lett.* **47**, 1588 (1981).

¹²J. J. Leventhal, *J. Chem. Phys.* **54**, 3279 (1971).

¹³V. Páca, U. Haveman, Z. Herman, F. Schneider, and L. Züllick, *Chem. Phys. Lett.* **49**, 273 (1977).

¹⁴N. Sathyamurthy, J. W. Duff, C. Stroud, and L. M. Raff, *J. Chem. Phys.* **67**, 3563 (1976).

¹⁵C. Zuhrt, F. Schneider, and L. Züllick, *Chem. Phys. Lett.* **43**, 571 (1976).

¹⁶P. J. Kuntz, *Chem. Phys. Lett.* **16**, 581 (1972).

¹⁷F. M. Chapman, Jr. and E. F. Hayes, *J. Chem. Phys.* **62**, 4400 (1975).

¹⁸F. Schneider, U. Havemann, L. Züllick, V. Páca, K. Birkinshaw, and Z. Herman, *Chem. Phys. Lett.* **37**, 323 (1976).

¹⁹D. J. Kouri and M. Baer, *Chem. Phys. Lett.* **24**, 37 (1974).

²⁰N. Sathyamurthy, R. Rangarajan, and L. M. Raff, *J. Chem. Phys.* **64**, 4606 (1976); C. Stroud, N. Sathyamurthy, R. Rangarajan, and R. M. Raff, *Chem. Phys. Lett.* **48**, 350 (1975).

²¹J. T. Muckerman, *J. Chem. Phys.* **54**, 115 (1971); **56**, 2997 (1972).